# Porphyrin Electrode Films Prepared by Electrooxidation of Metalloprotoporphyrins

**K. A. Macor and T. G. Spiro***

*Contribution from the Department of Chemistry, Princeton University, Princeton, New Jersey 08544.* *Received February 2, 1983*

**Abstract:** Electrooxidation in organic solvents of the dimethyl esters of several metalloprotoporphyrins (PP) ($Ni^{II}PP$, $Zn^{II}PP$, $Co^{II}PP$, $(Fe^{III}PP)Cl$, $(Fe^{III}PP)_2O$, and $(Cr^{III}PP)_2O$) leads to the deposition of thick (~1000 monolayer equivalents), electroactive porphyrin films, which have been characterized by cyclic voltammetry and absorption spectroscopy on transparent $SnO_2$ electrodes. The films are stable toward organic solvents and aqueous acids and bases, but are removed by treatment with hot concentrated acids. The resonance Raman spectrum of the NiPP film indicates that one of the two vinyl groups is saturated on most of the porphyrin units. Deposition continues for some minutes after the current is interrupted. This evidence is consistent with a mechanism involving electroinitiated cationic vinyl polymerization. No film is formed if the metal, rather than the ring, is oxidized. Thus the first oxidation step of $Co^{II}PP$, to $[Co^{III}PP]^+$, does not support film formation (although the potential is as high as for ring oxidation in ZnPP), but the second step, to $[Co^{III}PP\cdot]^{2+}$, does. Lack of film formation for $(Mn^{III}PP)Cl$ and $(Cr^{IV}PP)O$ suggests metal, rather than ring oxidation, to $Mn^{IV}$ and $Cr^{V}$. However, $(CrPP)_2O$ oxidation does produce a film, suggesting ring oxidation, analogous to $(FePP)_2O$, which also produces a film. However, while $(CrPP)_2O$ is incorporated intact into the film, the $(FePP)_2O$ film contains monomer units. Incorporation of other metal ions can be accomplished by soaking a ZnPP-coated electrode in $H_2SO_4$ followed by contact with a solution of the metal dihalide in refluxing DMF. The porphyrin sites are accessible to small ions, as shown by chloride coordination of ZnPP film upon soaking in chloride solution.

## Introduction

There is much current interest in the attachment of electroactive molecules to electrode surfaces, with the aim of catalyzing desirable electrode reactions and inhibiting undesirable ones.[1-9] In the case of semiconductor photoelectrodes, attachment of chromophoric molecules can also provide photosensitization.[10,11] In earlier work from this laboratory, chemistry was developed for the introduction of vinyl groups into the aromatic rings of $[Ru(bpy)_3]^{2+}$ (bpy = 2,2'-bipyridine) complex[12] whose photophysical properties have made it the focus of much attention in chemical schemes for solar energy conversion,[13,14] and also $[Ru(phen)_3]^{2+}$,[15] (phen = *o*-phenanthroline). These vinyl complexes were attached to electrode surfaces via hydrosilylation and condensation with surface hydroxyl groups, and the resulting films were shown to be electroactive, and to provide photosensitization of n-type $SnO_2$, albeit with low quantum efficiency.[12] Subsequently Murray and co-workers[16] showed that vinyl$[Ru(bpy)_3]^{2+}$ and related complexes could be induced to form stable electroactive films simply by cycling the electrode over the reduction wave of the complex. The added electron enters a $\pi^*$ orbital of the aromatic ligand and apparently imparts sufficient anion character to the conjugated vinyl groups to initiate anionic polymerization.[16] The mode of attachment of the resulting polyvinyl complexes to the electrode surfaces is unknown, but the films do adhere quite strongly, provided that the solvent from which the complexes are deposited is not also a good solvent for the polymers. The electrochemical properties of these films have been studied extensively.[15-19]

We have been attracted to the idea of using a similar approach to the attachment of metalloporphyrins to electrodes. These molecules are electroactive, are even better photosensitizers than $[Ru(bpy)]^{2+}$ (absorbing light further to the red), and have the advantage of allowing coordination of additional ligands to the central metal ion, above and below the porphyrin plane. They offer the possibility of combining electron transfer with ligand redox chemistry, with stabilization of otherwise highly energetic redox products, e.g., H and O atoms. Thus rational schemes for catalyzing useful electrode reactions can in principle be devised. Previous studies of porphyrins and phthalocyanines at electrode surfaces have relied on simple adsorption,[1,6,9] vapor deposition,[20,21] or condensation reactions of porphyrin side chains with functionalized electrodes.[22,23] It is difficult by these means to obtain stable electroactive films which allow access to the central metal ion by reactants in solution. It happens that protoporphyrin IX, the most ubiquitous naturally occurring porphyrin (present in hemoglobin, myoglobin, peroxidases, and b-type cytochromes), has two vinyl side chains (see Figure 1), conjugated to the porphyrin $\pi$ system. We decided to determine whether these vinyl groups could be used for electroinitiated polymerization, analogous to the results with vinyl$[Ru(bpy)_3]^{2+}$. It turned out that electrode cycling over the protoporphyrin reduction waves does not lead to film formation, but cycling over oxidation waves does produce films in those cases where the oxidation is reversible and plausibly leads to porphyrin radical-cation formation. These results and the characterization of the metalloprotoporphyrin films are the subject of this article.

## Experimental Section

**Preparation of Metalloporphyrin Complexes.** Metalation of protoporphyrin dimethyl ester and mesoporphyrin dimethyl ester (Mid-Century, Inc., Pozen, IL) was carried out by the method of Adler.[24]

(1) Zagal, J.; Sen, R. K.; Yeager, E. *J. Electroanal. Chem.* **1977**, *83*, 207.
(2) Evans, J. F.; Kuwana, T.; Henne, M. T.; Royer, G. P. *J. Electroanal. Chem.* **1977**, *80*, 409.
(3) Tse, C. S.; Kuwana, T. *Anal. Chem.* **1978**, *50*, 1315.
(4) Kerr, J. B.; Miller, L. L. *J. Electroanal. Chem.* **1979**, *101*, 623.
(5) Bettelheim, A.; Chan, R. J.; Kuwana, T. *J. Electroanal. Chem.* **1980**, *110*, 93.
(6) Collman, J. P.; Denisevich, P.; Konai, Y.; Morrocco, M.; Koval, C.; Anson, F. C. *J. Am. Chem. Soc.* **1980**, *102*, 6027.
(7) Abruna, H. D.; Walsh, J. L.; Meyer, T. J.; Murray, R. W. *J. Am. Chem. Soc.* **1980**, *102*, 3272.
(8) Samuels, G. J.; Meyer, T. J. *J. Am. Chem. Soc.* **1981**, *103*, 307.
(9) Shigehara, K.; Anson, F. C. *J. Phys. Chem.* **1982**, *86*, 2776.
(10) Gerischer, H. *Photochem. Photobiol.* **1972**, *16*, 243.
(11) Clark, W. D.; Sutin, N. *J. Am. Chem. Soc.* **1977**, *99*, 4676.
(12) Ghosh, P. K.; Spiro, T. G. *J. Am. Chem. Soc.* **1980**, *102*, 5543.
(13) Brown, G. M.; Brunschwig, B. S.; Creutz, C.; Endicott, J. F.; Sutin, N. *J. Am. Chem. Soc.* **1979**, *101*, 1298.
(14) DeLaire, P. J.; Sullivan, B. P.; Meyer, T. J.; Whitten, D. G. *J. Am. Chem. Soc.* **1979**, *101*, 4007.
(15) Ghosh, P. K.; Spiro, T. G. *J. Electrochem. Soc.* **1981**, *128*, 1281.
(16) Abruna, H. D.; Denisevich, P.; Umana, M.; Meyer, T. J.; Murray, R. W. *J. Am. Chem. Soc.* **1981**, *103*, 1.
(17) Umana, M.; Denisevich, P.; Rolison, D. R.; Nakahama, S.; Murray, R. W. *Anal. Chem.* **1981**, *53*, 1170.
(18) Ikeda, T.; Leidner, C. R.; Murray, R. W. *J. Am. Chem. Soc.* **1981**, *103*, 7422.
(19) Denisevich, P.; Abruna, H. D.; Leidner, C. R.; Meyer, T. J.; Murray, R. W. *Inorg. Chem.* **1982**, *21*, 2153.
(20) Tachikawa, H.; Faulkner, L. *J. Am. Chem. Soc.* **1978**, *100*, 4379.
(21) Jaeger, C.; Fan, F.; Bard, A. J. *J. Am. Chem. Soc.* **1980**, *102*, 2592.
(22) (a) Jester, C. P.; Rocklin, R. D.; Murray, R. W. *J. Electrochem. Soc.* **1980**, *127*, 1979. (b) Willman, K. W.; Rocklin, R. D.; Nowak, R.; Kuo, K. N.; Schultz, F. A.; Murray, R. W. *J. Am. Chem. Soc.* **1980**, *102*, 7629.
(23) Elliott, C. M.; Marresse, C. A. *J. Electroanal. Chem.* **1981**, *119*, 395.
(24) Adler, D. A.; Longo, F. R.; Kampas, F.; Kim, J. *J. Inorg. Nucl. Chem.* **1970**, *32*, 2443.

0002-7863/83/1505-5601$01.50/0 

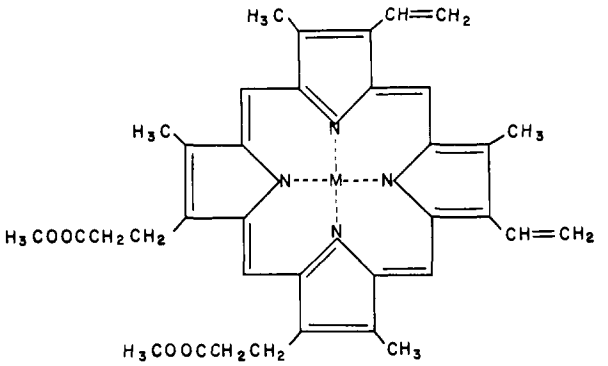


**Figure 1.** Structure of metalloprotoporphyrin dimethyl ester. In mesoporphyrin dimethyl ester the vinyl side chains are replaced with ethyl groups.

$\mu$-Oxo dimer complexes of iron protoporphyrin dimethyl ester and iron mesoporphyrin dimethyl ester were prepared by shaking a $CH_2Cl_2$ solution of the $Cl^-$ or $Br^-$ monomer with 1 M KOH several times until the characteristic charge-transfer band of the monomer in the region of 630 nm disappeared.

$\mu$-Oxo dimer chromium protoporphyrin dimethyl ester was prepared by placing freshly made chromium protoporphyrin dimethyl ester chloride on a grade III alumina column. Prior to elution of the $\mu$-oxo dimer, any oxo-chromium protoporphyrin dimethyl ester present (which forms during isolation of the chromium protoporphyrin dimethyl ester chloride complex) was eluted with $CH_2Cl_2$ as a red band with a Soret peak at 398 nm. The $\mu$-oxo dimer was then eluted with ethanol as a brownish green band with a Soret peak at 420 nm. Formation of the $\mu$-oxo complex was verified by a molecular weight determination (1298 g/mol calcd; 1277 g/mol found).

**Electrochemical Instrumentation and Procedures.** Cyclic voltammetry was carried out with a PAR Model 173 potentiostat, 175 programmer, and 179 coulometer. Voltammograms were recorded on an X-Y recorder. A saturated calomel electrode was used as the reference electrode.

The metalloporphyrins films were formed by electrochemical cycling through the metalloporphyrin oxidation waves or by potentiostating the working electrode [Pt, $SnO_2$ (PPG Ind., Pittsburgh, PA) or glassy carbon (Normar Ind., Anaheim, CA)] at a potential sufficiently positive to oxidize the metalloporphyrin.

**Spectroscopy.** Raman spectra were obtained with a cw $Kr^+$ (4067 Å) laser with the samples in back-scttering geometry, and recorded with a Spex 1401 double monochromator with a photomultiplier and photon-counting electronics.

Absorption spectra of optically transparent $SnO_2$ electrodes were obtained with a Cary 118 spectrophotometer.

## Results

**A. Electrode Film Formation from Metalloprotoporphyrins.** The electrochemical characteristics of $Zn^{II}$, $Ni^{II}$, $Co^{II}$, $Fe^{III}$, $Cr^{III}$, $Cr^{IV}$, and $Mn^{III}$ complexes of protoporphyrin IX dimethyl ester (PP; see Figure 1 for the porphyrin structure) in methylene chloride ($CH_2Cl_2$) or butyronitrile (PrCN) were investigated via cyclic voltammetry at a Pt electrode. Reductive scanning produced well-behaved waves due to reduction of the metal and/or the porphyrin ring,[25] but oxidative scanning often produced waves which grew in size upon successive scans and deposited porphyrin on the electrode, as evidenced by a steadily deepening color.

Figure 2 shows the oxidative peaks of NiPP; the current grows incrementally with each successive scan. A film of NiPP can also be formed by allowing current to flow at potentials within the oxidative peak. In contrast the same peak for NiMP (MP = mesoporphyrin IX dimethyl ester) shows no growth in current on successive scans (Figure 2). The only difference between PP and MP is that the vinyl groups of PP are replaced with ethyl groups in MP (see Figure 1). It is clear that vinyl groups are directly responsible for the formation of the NiPP film.

The absorption spectrum of NiPP film grown on a transparent $SnO_2$ electrode is compared with those of NiPP and NiMP in $CH_2Cl_2$ solution in Figure 3. The three absorption bands are

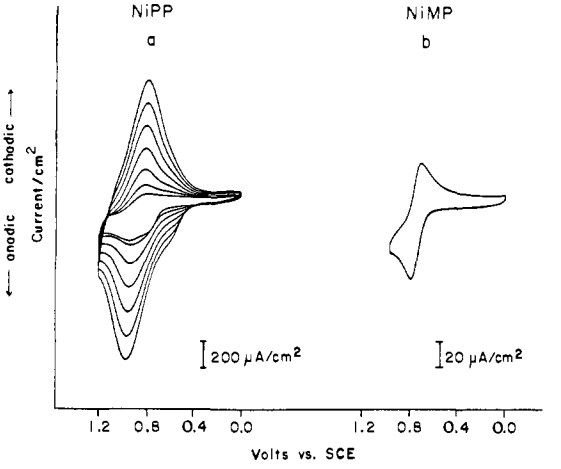


**Figure 2.** Consecutive cyclic voltammetric scans at Pt electrodes of (a) 0.5 mM NiPP in 0.1 M TBAP/$CH_2Cl_2$ at 200 mV/s and (b) 0.5 mM NiMP in 0.1 M TBAP/PrCN at 200 mV/s.

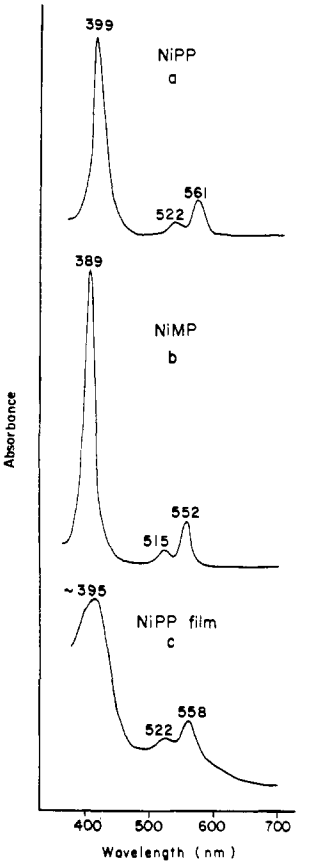


**Figure 3.** Absorption spectra of (a) NiPP in $CH_2Cl_2$, (b) NiMP in $CH_2Cl_2$, and (c) NiPP film on transparent $SnO_2$ in $CH_2Cl_2$.

associated with the B (Soret) and $Q_1$, and $Q_0$ ($\beta$ and $\alpha$) $\pi - \pi^*$ transitions of the porphyrin dianion.[26] They are red-shifted by ~10 nm for NiPP, relative to NiMP, owing to the vinyl group conjugation. The film absorption bands are slightly (~3 nm) blue-shifted from NiPP, and are appreciably broader, reflecting heterogeneity of the porphyrin sites in the film (perhaps due to variable axial interactions between the $Ni^{II}$ ions and the carbonyl groups of nearby ester peripheral substituents; see Figure 1), and/or excitonic interactions among neighboring chromophores. The latter are expected to influence the strong B band particularly,[27] and the B band of the film is observed to be markedly

(25) Felton, R. H. In "The Porphyrins"; Dolphin, D., Ed.; Academic Press: New York, 1978; Vol. V, pp 53–125.

(26) Gouterman, M. In ref 25, Vol. III, pp 1–165.

(27) Selensky, R.; Holten, D.; Windsor, M.; Paine, J. B.; Dolphin, D. D. *Chem. Phys.* **1980**, *60*, 33.

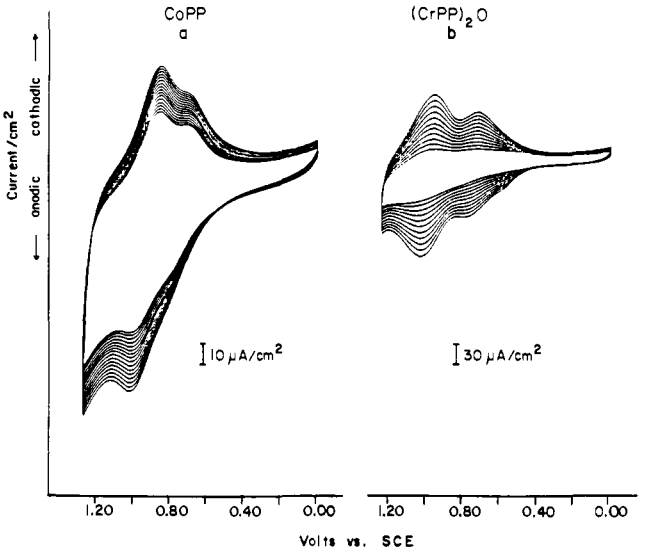


**Figure 4.** Consecutive cyclic voltammetric scans at Pt electrodes of (a) 0.5 mM CoPP in 0.1 M TBAP/$CH_2Cl_2$ at 200 mV/s and (b) 0.5 mM $(CrPP)_2O$ in 0.1 M TBAH/$CH_2Cl_2$ at 100 mV/s.

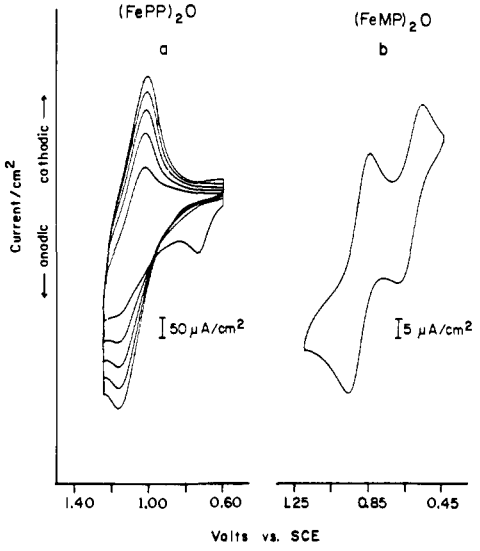


**Figure 5.** Consecutive cyclic voltammetric scans at Pt electrodes of (a) 0.5 mM $(FePP)_2O$ in 0.1 M TBAH/$CH_2Cl_2$ at 50 mV/s and (b) 0.5 mM $(FeMP)_2O$ in 0.1 M TBAH/$CH_2Cl_2$ at 50 mV/s.

broadened. When the film is dried in air, the bands shift ~3 nm to the red, presumably reflecting the intensification of axial and excitonic interactions due to solvent removal; the red shift is reversed when the film is contacted with solvent. These interactions are superimposed upon the spectral effect of partially saturating the peripheral vinyl groups for which there is independent evidence from Raman spectroscopy (see below).

Figure 4 shows oxidative voltammetric peaks for $Co^{II}PP$ and for $(Cr^{III}PP)_2O$, which also form electrode films, albeit at a slower rate than for NiPP. Likewise, film formation is observed for $Zn^{II}PP$, $(Fe^{III}PP)Cl$, and $(Fe^{III}PP)_2O$, but not for $(Mn^{III}PP)Cl$ or for $(Cr^{IV}PP)O$. $Co^{II}PP$ shows two oxidation waves, corresponding to oxidation of $Co^{II}$ to $Co^{III}$, and then oxidation of the porphyrin ring to the radical cation.[28] If the potential is increased only to the $Co^{III/II}$ wave, no film is formed. Two waves are also found for $(Cr^{III}PP)_2O$; the site of oxidation has not been studied for this complex. Again the first wave does not support film formation, but the second does.

Figure 5 shows oxidative scans for $(Fe^{III}PP)_2O$ and for $(Fe^{III}MP)_2O$. Two waves are again observed, as they are for the $\mu$-oxo dimer of several $Fe^{III}$ porphyrins.[29,30] These have been the

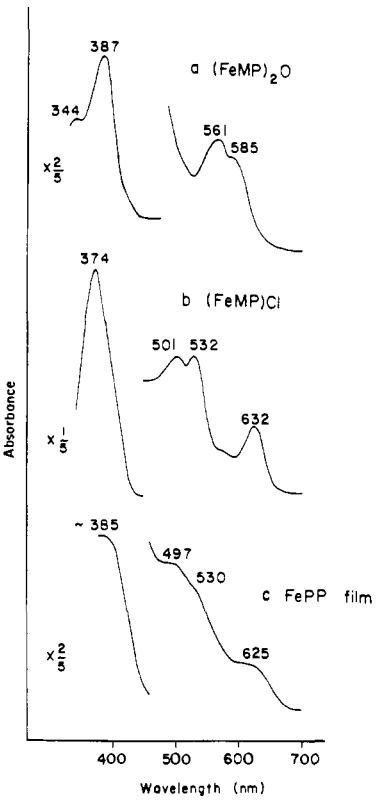


**Figure 6.** Absorption spectra of (a) $(FeMP)_2O$ in $CH_2Cl_2$, (b) (FeMP)Cl in $CH_2Cl_2$, and (c) FePP film (from $(FePP)_2O$ electrooxidation) on transparent $SnO_2$ in $CH_2Cl_2$.

subject of a number of studies, and of controversy with respect to the site of oxidation.[29-34] The most recent evidence favors ring oxidation in both waves.[31-34] While the $(Fe^{III}MP)_2O$ voltammogram is well behaved, that of $(Fe^{III}PP)_2O$ shows striking alterations upon successive scans. The second wave grows steadily and is accompanied by film formation, but the first wave diminishes sharply after the first scan and thereafter gradually disappears. Moreover the absorption spectrum of the $(Fe^{III}PP)_2O$ film on $SnO_2$ (Figure 6) is characteristic of a monomeric high-spin $Fe^{III}$ porphyrin, not a $\mu$-oxo dimer. The former species have a band in the ~620-nm region, assigned to a porphyrin $\rightarrow Fe^{III}$ charge-transfer transition,[35] whereas the latter show strongly red-shifted $Q_0$ and $Q_1$ bands and no charge-transfer band (Figure 6). The film spectrum shows visible peaks at wavelengths quite close to those of $(Fe^{III}MP)Cl$ (the B band position is uncertain because of strong glass absorption below 400 nm). The charge-transfer band intensity is sensitive to the nature of the axial ligand;[36] the weak band seen in the film spectrum is reminiscent of that observed for acetate complexes[37] and suggests that the ester peripheral groups may provide axial ligation to the monomeric FePP units in the film. These results establish that $(Fe^{III}PP)_2O$ dissociates into monomeric units when it forms a film upon oxidation; it happens that the single wave of the monomeric units falls at the same potential as the second wave of $(Fe^{III}PP)_2O$. The loss of the first wave upon successive scanning means that the film

(28) Wolberg, A.; Manassen, J. *J. Am. Chem. Soc.* **1970**, *92*, 2982.

(29) Felton, R. H.; Owen, G. S.; Dolphin, D.; Forman, A.; Borg, D. C.; Fajer, J. *Ann. N.Y. Acad. Sci.* **1973**, *206*, 504.
(30) Kadish, K.; Cheng, J.; Cohen, S.; Summerville, D. *ACS Symp. Ser.* **1976**, *38*, 65.
(31) Phillippi, M. A.; Goff, H. M. *J. Am. Chem. Soc.* **1979**, *101*, 7641.
(32) Phillippi, M. A.; Shimomura, E. T.; Goff, H. M. *Inorg. Chem.* **1981**, *20*, 1322.
(33) Shimomura, E. T.; Phillippi, M. A.; Goff, H. M. *J. Am. Chem. Soc.* **1981**, *103*, 6778.
(34) English, D. R.; Hendrickson, D. N.; Suslick, K. S. *J. Am. Chem. Soc.*, submitted for publication.
(35) Adar, F. In ref 26, pp 167–209.
(36) Smith, D. W.; Williams, R. J. *Struct. Bonding (Berlin)* **1970**, *7*, 1.
(37) Smith, D. W.; Williams, R. J. *Biochem. J.* **1968**, *110*, 297.

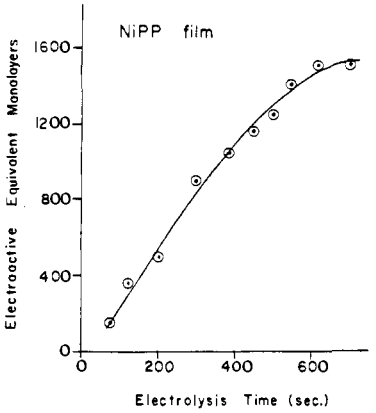


**Figure 7.** Plot of NiPP monolayer equivalents (as determined from integration of the cyclic voltammetric current) vs. the electrolysis time at 1.05 V vs. SCE.

Table I. Metalloprotoporphyrin Oxidations

| metallo-proto-porphyrin | electro-lytic anion | $\xi^{1/2}$ (V vs. SCE) | redox process[a] | film forma-tion |
|---|---|---|---|---|
| ZnPP | $ClO_4^-$ | 0.75 | $PZn^{II} \overset{e^-}{\rightleftharpoons} P^{+}\cdot Zn^{II}$ | yes |
| CoPP | $ClO_4^-$ | 0.74 | $PCo^{II} \overset{e^-}{\rightleftharpoons} PCo^{III}$ | no |
| | | 0.93 | $PCo^{III} \overset{e^-}{\rightleftharpoons} P^{+}\cdot Co^{III}$ | yes |
| NiPP | $ClO_4^-$ | 0.93 | $PNi^{II} \overset{e^-}{\rightleftharpoons} PNi^{III} \rightleftharpoons P^{+}\cdot Ni^{II}$ | yes |
| | | 1.1 | $P^{+}\cdot Ni^{II} \rightleftharpoons P^{2+}Ni^{II}$ | |
| (CrPP)O | $ClO_4^-$ | 0.91 | | no |
| (FePP)Cl | $ClO_4^-$ | 1.08 | | yes |
| (MnPP)Cl | $ClO_4^-$ | 1.12 | | no |
| $(CrPP)_2O$ | $PF_6^-$ | 0.75 | | no |
| | | 0.99 | | yes |
| $(FePP)_2O$ | $PF_6^-$ | 0.79 | | very slight |
| | | 1.07 | | yes |

[a] Accepted assignments based upon EPR and absorption spectral data.[28,38,39]

inhibits the incoming $(Fe^{III}PP)_2O$ molecules from reaching the electrode surface and being oxidized directly. Film growth must be via interaction of the oxidized monomeric units already deposited with $(Fe^{III}PP)_2O$ molecules in solution.

Voltammograms of protoporphyrin free base (not shown) show broad oxidation waves centered at ~0.9 V, which sharpen only if the scan rate is increased to quite high values (1000 mV/s). This irreversibility presumably reflects rapid decomposition reactions of the oxidation product. No film formation is observed upon successive scanning.

The metalloprotoporphyrin oxidation potentials and film-forming properties are summarized in Table I.

**B. Film Growth and Electrochemistry.** Figure 7 shows the progress of $Ni^{II}PP$ film formation when a Pt electrode in a 0.5 mM solution of $Ni^{II}PP$ in $TBAP/CH_2Cl_2$ was held at a potential, 1.05 V vs. SCE, within the oxidation wave. The electrolysis was interrupted periodically and the amount of electroactive material was determined by cyclic voltammetry. The total electroactive material increased steadily to $1.5 \times 10^{-7}$ mol/cm$^2$, after which no further deposition was observed. This amount corresponds to about 1500 monolayers, if the porphyrin units are assumed to lie flat and occupy 170 Å$^2$ of surface area (estimated from the distance from the center of the ring to the second carbon atom of the peripheral substituents); it is unlikely, however, that the molecules do lie flat, or that the film grows in uniform layers. For $Zn^{II}PP$, $Co^{II}PP$, $(Cr^{III}PP)_2O$, and $(Fe^{III}PP)_2O$, the limiting film thickness was about half that observed for NiPP.

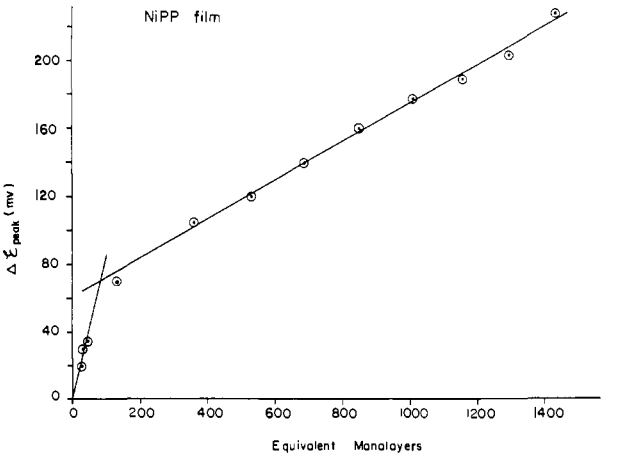


**Figure 8.** Plot of voltammetric peak separation vs. the number of monolayer equivalents (as determined from integration of the cyclic voltammetric current).

In a separate experiment the amount of current passed at 1.2 V vs. SCE was measured and compared with the amount of electroactive material deposited. The ratio was found to be close to 1.0, independent of the concentration of $Ni^{II}PP$. This ratio indicates that essentially every NiPP molecule that is oxidized is incorporated into the film.

As the film grows thicker the voltammograms become progressively less reversible, as judged by increasing separation of the anodic and cathodic peak potentials (which should be zero for fully reversible redox processes of surface localized species), reflecting increasing times for electron transfer through the film. Interestingly, an initial sharp increase in the peak-to-peak separation at low coverage (Figure 8) is followed by a slower increase at greater coverage, which is linear with thickness over 100–1500 monolayer equivalents. The initial portion of the curve extrapolates to zero, as expected for ideal behavior at zero coverage. Apparently the factors leading to irreversibility (presumably associated with porphyrin units poorly oriented for electron migration through the film) become less consequential, per unit of film thickness, at higher coverage, with an abrupt change at about 100 monolayer equivalents.

An observation relevant to the mechanism of film formation is that the amount of electroactive material continued to increase for a time after the current was interrupted. In one set of experiments on Pt electrodes with $\sim 3 \times 10^{-8}$ mol/cm$^2$ coverage, the incremental growth as judged by voltammetry in fresh electrolyte was 22, 32, and 36% after 1, 3, and 8 min of standing in the NiPP solution after interruption of the plating current. A second voltammogram in the fresh electrolyte showed that about half of the incremental electroactive material was lost to the solution, but the rest remained on the electrode through successive scans.

**C. Role of the Electrolyte Anion.** Figure 9 shows a substantial effect on film formation of the nature of the supporting electrolyte. When tetrabutylammonium perchlorate (TBAP) is used, NiPP shows two overlapping anodic waves, separated by ~0.10 V; both waves grow in parallel as the film grows. When tetrabutylammonium hexafluorophosphate (TBAH) is used instead, the two waves are initially separated by ~0.4 V, but as the film grows the waves merge into a pattern similar to that observed when TBAP is the electrolyte.

The initial NiPP voltammograms are similar (though displaced toward lower potentials) to those observed for NiTPP (TPP = tetraphenylporphine) by Dolphin and co-workers,[39] who were able to determine via EPR and optical spectroscopy that in $TBAP/CH_2Cl_2$, oxidation of $Ni^{II}TPP$ led initially to $[Ni^{III}TPP]^+$, which rapidly decayed to $[Ni^{II}TPP\cdot]^+$, whereas in $TBAH/CH_2Cl_2$, $[Ni^{II}TPP\cdot]^+$ was formed directly. (The ~0.3-V peak separation

(38) Fajer, J.; Borg, D. C.; Forman, A.; Felton, R. H.; Vegh, L.; Dolphin, D. *Ann. N.Y. Acad. Sci.* **1973**, *206*, 349.
(39) Johnson, E. C.; Niem, T.; Dolphin, D. *Can. J. Chem.* **1978**, *56*, 1381.

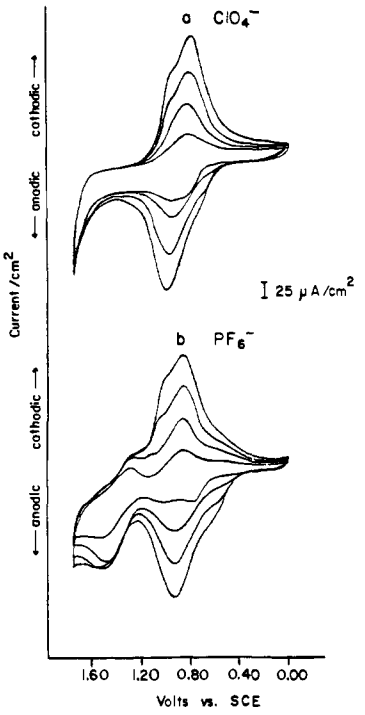


**Figure 9.** Consecutive cyclic voltammetric scans at Pt electrodes of 0.5 mM NiPP in (a) 0.1 M TBAP/$CH_2Cl_2$ and (b) 0.1 M TBAH/$CH_2Cl_2$ at 100 mV/s.

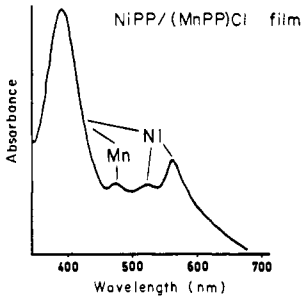


**Figure 10.** Absorption spectrum of $SnO_2$ electrode after potential scanning in 0.5 mM NiPP/0.5 mM (MnPP)Cl in 0.1 M TBAP/$CH_2Cl_2$.

observed in TBAH is characteristic of the potential difference between porphyrin mono- and dication formation.) Presumably $ClO_4^-$ is a slightly better ligand than $PF_6^-$ and is able to stabilize $Ni^{III}$ transiently. The merging of the waves in successive TBAH scans probably reflects the availability of the porphyrin ester groups as axial ligands, resulting in $Ni^{III}$ stabilization and leading to voltammograms similar to those observed in TBAP.

A similar situation may obtain for $(Fe^{III}PP)_2O$ since film growth is observed to be much faster in TBAH than TBAP. Transient stabilization of $Fe^{IV}$ by $ClO_4^-$ could slow the rate of radical cation formation and retard film growth upon $(Fe^{III}PP)_2O$ oxidation.

**D. Codeposition of $Mn^{III}$ and $Ni^{II}$PP.** Although oxidation of $(Mn^{III}PP)Cl$ does not produce a film, this complex can be incorporated into a $Ni^{II}PP$ film, formed by oxidative cycling in a solution containing both complexes. Figure 10 shows that such a film formed on $SnO_2$ has an absorption spectrum with peaks derived from both $Mn^{III}$ and $Ni^{II}$ porphyrin. ($Mn^{III}$ porphyrins have distinctive long-wavelength bands in the Soret region, attributed to mixing of charge-transfer and $\pi-\pi^*$ transitions.[40]) The absorption peak heights indicate about 20% $Mn^{III}$ incorporation in the film, although the solution contained a 50–50 mixture of $(Mn^{III}PP)Cl$ and $Ni^{II}PP$.

**E. Replacement of $Zn^{II}$ in ZnPP Film with Other Metal Ions.** Soaking a ZnPP-coated electrode in $H_2SO_4$ followed by contact with $MnCl_2$ in refluxing DMF yielded (MnPP)Cl film. Replacement of $Zn^{II}$ with $Mn^{III}$ was verified by absorption spectroscopy on a $SnO_2$ electrode.

(40) Boucher, L. J. *J. Am. Chem. Soc.* **1970**, *92*, 2725.

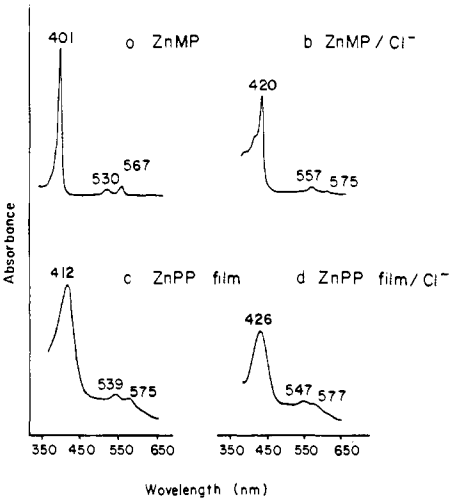


**Figure 11.** Absorption spectra of (a) ZnMP in $CH_2Cl_2$, (b) ZnMP in TBAC/$CH_2Cl_2$, (c) ZnPP film in $CH_2Cl_2$, and (d) ZnPP film in TBAC/$CH_2Cl_2$.

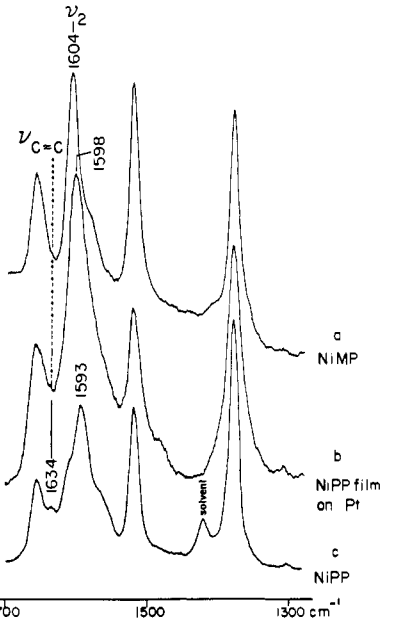


**Figure 12.** Resonance Raman spectra of NiMP in $CH_2Cl_2$, NiPP film on Pt, and NiPP in $CH_2Cl_2$ excited at 4067 Å. Conditions: laser power 100 mW, slit width 10 $cm^{-1}$, time constant 5 s, scanning speed 0.5 $cm^{-1}/s$.

**F. $Cl^-$ Complexation in $Zn^{II}$PP Film.** When a $Zn^{II}$PP-coated electrode, prepared by oxidative cycling in a TBAP/$CH_2Cl_2$ solution of $Zn^{II}PP$, is removed from this solution and placed in a solution of tetrabutylammonium chloride (TBAC) in $CH_2Cl_2$, the peak of its voltammogram is shifted from 0.75 to 0.54 V vs. SCE. This 210-mV downshift parallels that observed for $Zn^{II}MP$ in chloride vs. perchlorate medium and is attributable to coordination of the $Zn^{II}$ by chloride.[38] Moreover, the Soret absorption band of the $Zn^{II}PP$ film on $SnO_2$ shows a 14-nm red shift upon immersion in chloride solution (Figure 11), in parallel with the 19-nm red shift between perchlorate and chloride solutions observed for $Zn^{II}MP$, again attributable to chloride complexation.[38] (In the chloride solution the Soret band of the ZnPP film is broadened and red-shifted relative to ZnMP, presumably reflecting excitonic interactions. In the absence of chloride all of the film absorption bands are appreciably red-shifted, relative to ZnMP, probably reflecting the coordinating ability of the porphyrin ester groups.) Thus most of the $Zn^{II}$ ions in the film appear to be accessible to chloride ions from the solution. The thickness of the film was estimated electrochemically to contain 100 monolayer equivalents.

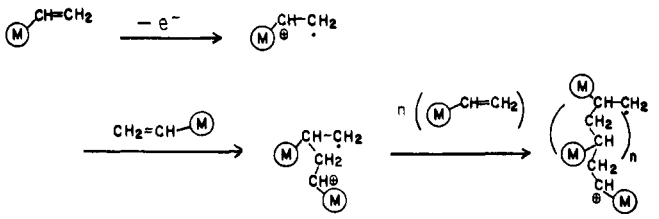

**Figure 13.** Scheme for proposed electrooxidative radical vinyl polymerization of metalloprotoporphyrins.

**G. Raman Characterization.** Raman spectra of a $Ni^{II}PP$-coated Pt electrode, removed from the generating solution and dried in air, were obtained via backscattering. Figure 12 shows the spectrum obtained with 4067-Å excitation, in resonance with the Soret absorption, and compares it with those of $Ni^{II}PP$ and $Ni^{II}MP$ in solution. The Raman spectra of these complexes have been analyzed and assigned.[41,42] Of particular interest are the $Ni^{II}PP$ bands at 1634 and 1593 $cm^{-1}$, which arise respectively from the C=C stretch, $\nu_{C=C}$, of the peripheral vinyl groups, and from a porphyrin skeletal model, $\nu_2$, which is coupled with $\nu_{C=C}$. In NiMP $\nu_{C=C}$ is absent, because of the replacement of vinyl with ethyl groups, and $\nu_2$ increases 11 $cm^{-1}$. In the $Ni^{II}PP$ electrode film the intensity of $\nu_{C=C}$ is diminished, while $\nu_2$ is 5 $cm^{-1}$ higher than in the $Ni^{II}PP$ spectrum. These changes are clear evidence for partial saturation of the vinyl groups. Because of the overlapping bands it is difficult to be quantitative about the degree of saturation, but the position of $\nu_2$, half-way between $Ni^{II}PP$ and $Ni^{II}MP$, suggests that one out of the two $Ni^{II}PP$ vinyl groups, on the average, are saturated in the film.

In view of recent interest in surface-enhanced Raman scattering (SERS),[43] the question naturally arises as to whether the electrode is enhancing the $Ni^{II}PP$ film spectrum (although SERS has not been observed on Pt surfaces). A calculation comparing the intensities of the strong band at 1380 $cm^{-1}$ and the concentrations of porphyrin molecules in the laser beam indicated that there were enough molecules in the film (estimated voltammetrically to be $10^{16}$ molecules/$cm^2$) to account for the observed signal without any surface enhancement.

## Discussion

The mechanism of metalloprotoporphyrin film formation is suggested to be radical-cation-initiated vinyl polymerization, as illustrated in Figure 13. Evidence in support of this mechanism includes the following observations.

(1) The vinyl groups are partially saturated in the film, as determined by Raman spectroscopy.

(2) Porphyrin deposition continues for a few minutes after the electrolysis current is shut off.

(3) A complex which does not by itself form a film, ($Mn^{III}$-PP)Cl, can nevertheless, be codeposited with a complex which does, $Ni^{II}PP$. This observation is readily explained by attack of the $Ni^{II}PP^{+\cdot}$ radical cation on ($Mn^{III}PP$)Cl, as well as $Ni^{II}PP$, in solution.

(4) No film is formed when oxidation is exclusively at the metal center, even if the potential is adequate in other cases. Thus, $Co^{II}PP$ does not form a film at the first anodic wave, corresponding to $Co^{III}PP$ formation, even though the potential, 0.75 V vs. SCE, is the same as that required to oxidize $Zn^{II}PP$ to its radical cation, with attendant film formation. Since the vinyl groups are conjugated with the porphyrin ring, they remain unactivated if no significant electron removal occurs at the ring.

(5) The rate of film formation increases with the rate of ring vs. metal oxidation. Thus TBAH electrolyte enhances film growth over TBAP for $(Fe^{III}PP)_2O$, plausibly because $ClO_4^-$ stabilizes $Fe^{IV}$ transiently relative to $PF_6^-$.

The question of metal vs. ring oxidation of metalloporphyrins has been the subject of much research because of its relevance to oxidative and electron-transfer chemistry in porphyrin-containing biological systems.[44] The case of $Ni^{II}TPP$ is particularly revealing with respect to the possibility of competition between these two oxidative pathways. Not only does $Ni^{III}TPP$ form transiently and decay to $Ni^{II}TPP^{+\cdot}$ in the presence of $ClO_4^-$ but not $PF_6^-$, but at 77 K, an equilibrium between these two forms has been demonstrated.[39] More recently, attention has focussed on iron porphyrins, which are the prosthetic group of heme proteins. Although initial studies suggested $Fe^{III}$ oxidation to $Fe^{IV}$, analogous to the situation in peroxidases and catalase, recent evidence points to $Fe^{III}$ radical cation as the dominant species in most cases,[31-34,45-47] even for the relatively low-potential (~0.75 V) first oxidation of $\mu$-oxo $Fe^{III}$ porphyrin dimers.[31-34]

Like $(Fe^{III}PP)_2O$, $(Cr^{III}PP)_2O$ supports ready film formation, implicating radical-cation formation at least in the second wave (0.99 V vs. SCE). On the other hand, $(Cr^{IV}PP)O$ does not form a film when cycled over its oxidation wave at 0.91 V vs. SCE. We conclude that this oxidation step involves formation of $[(Cr^{V}PP)O]^+$ primarily (perhaps with a $ClO_4^-$ axial ligand). There is good chemical precedent for the formation of oxo-$Cr^V$ porphyrin.[48,49] The striking difference between $(Cr^{III}PP)_2O$ and $(Cr^{IV}PP)O$ in this regard must reflect the ability of a bare oxo ligand to stabilize high oxidation states of the metal ion to which it is bound. When $O^{2-}$ serves as a bridging ligand this ability seems to be greatly diminished. It also appears that $(Mn^{III}PP)Cl$ is oxidized mainly to $[(Mn^{IV}PP)Cl]^+$, since no film is obtained.

For $(Fe^{III}PP)_2O$, the situation is complicated by the breakdown of the complex into monomeric units upon film formation, as evidenced both by the voltammogram and the absorption spectrum of the film. This behavior was unexpected, since the $\mu$-oxo dimer is a stable species, and the voltammogram of $(Fe^{III}MP)_2O$ is well behaved, showing no evidence of decomposition. Monomerization is therefore associated specifically with the film formation reaction. One possibility is that the polymerization process imposes steric strain on the dimeric complex sufficient to induce its dissociation. Another, more attractive possiblity is that polymerization brings one end of the dimer into contact with a coordinating ester group which induces displacement of a ferryl complex, $(Fe^{IV}PP)O$, upon removal of another electron, viz.

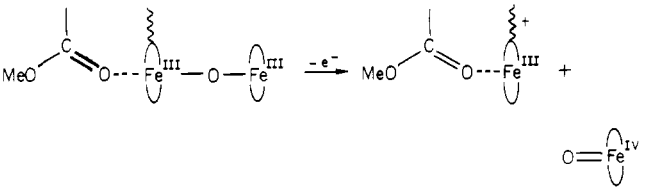

This reaction chemistry is applicable to $(Cr^{III}PP)_2O$ as well, but since $Cr^{III}$ complexes are less labile than $Fe^{III}$, it is plausible that the displacement reaction would be sufficiently slowed down to allow incorporation of the intact dimer into the polymeric film.

Many details of the polymerization reaction remain to be elucidated. One question relates to whether one or both of the vinyl groups of each protoporphyrin are involved. The Raman spectrum of the NiPP film suggests that half the vinyl groups are saturated, since the skeletal mode $\nu_2$ is found half-way between the NiMP and NiPP frequencies. If half-saturation represented a statistical average, then multiple bands, or a significantly

(41) Choi, S.; Spiro, T. G.; Langry, K. C.; Smith, K. M. *J. Am. Chem. Soc.* **1982**, *104*, 4337.
(42) Verna, A. L.; Mendelsohn, R.; Bernstein, H. J. *J. Chem. Phys.* **1974**, *61*, 383.
(43) Van Duyne, R. P. In "Chemial and Biochemical Applications of Lasers"; Moore, C. B., Ed.; Academic Press: New York, 1979; Vol. IV, pp 101-185.
(44) Dolphin, D.; Muljiani, Z.; Rousseau, K.; Borg, D. C.; Fajer, J.; Felton, R. H. *Ann. N.Y. Acad. Sci.* **1973**, *206*, 177.
(45) Gans, P.; Marchon, J. C.; Reed, C. A.; Regnard, J. R. *Nouv. J. Chim.* **1981**, *5*, 203.
(46) Scholz, W. F.; Reed, C. A.; Lee, Y. J.; Scheidt, W. R.; Lang, G. *J. Am. Chem. Soc.* **1982**, *104*, 6791.
(47) Buisson, G.; Deronzier, A.; Duee, E.; Gans, P.; Marchon, J. C.; Regnard, J. R. *J. Am. Chem. Soc.* **1982**, *104*, 6793.
(48) Groves, J. T.; Kruper, W. *J. Am. Chem. Soc.* **1979**, *101*, 7613.
(49) Groves, J. T.; Haushalter, R. C. *J. Chem. Soc. Chem. Commun.* **1981**, 1165.

broadened band, would be expected. This is not observed, suggesting that most of the porphyrin units in the film have one saturated and one intact vinyl group and that the degree of cross-linking is low. Whether the apparent deactivation of the second vinyl group should be attributed to steric or electronic effects is uncertain.

We do not know how the polymer is attached to the electrode surface, nor what the distribution of chain lengths is. The fact that a fraction of the electroactive material is lost when an electrode with preformed film is placed in fresh electrolyte and its voltammogram successively cycled suggests that at least some of the polymer segments are relatively small and dissociate readily from the rest of the film.

In this work we have shown that stable adherent metalloporphyrin films, showing good electroactivity over substantial thicknesses (>1000 monolayer equivalents), can be prepared by oxidative electropolymerization of metalloprotoporphyrin complexes. The reaction depends on ring oxidation of the porphyrin, as expected if the mechanism is cationic vinyl polymerization, and the considerable variations encountered among different complexes can largely be understood on the basis of differing degrees of ring vs. metal oxidation at the relevant potentials. The metalloporphyrin sites are accessible at least to small ions, as evidenced by facile chloride binding to the ZnPP film, and should be capable of carrying out redox chemistry on coordinated ligands. This chemistry is currently under investigation.

**Acknowledgment.** We thank Joseph R. Perno for work with chromium protoporphyrins and Lisa A. Miller for experiments on replacement of $Zn^{2+}$ in zinc protoporphyrin films. This work was supported by Grant DOE-AC02-81ER10861 from the U.S. Department of Energy.

**Registry No.** ZnPP, 15304-09-3; CoPP, 14932-10-6; NiPP, 15304-70-8; (CrPP)O, 86238-33-7; (FePP)Cl, 15741-03-4; (MnPP)Cl, 86238-34-8; $(CrPP)_2O$, 86259-39-4; $(FePP)_2O$, 36655-90-0; NiMp, 15892-09-8; $(FeMP)_2O$, 58280-33-4; (FeMP)Cl, 14126-91-1; FePP, 18922-89-9; $SnO_2$, 18282-10-5; Mn, 7439-96-5; Zn, 7440-66-6; Pt, 7440-06-4; TBAP, 1923-70-2; TBAH, 3109-63-5; TBAC, 1112-67-0.

# Bioorganic Applications of Mass Spectrometry. 3.[1] Fast-Atom-Bombardment-Induced Zwitterionic Oligonucleotide Quasimolecular Ions Sequenced by MS/MS

**Maria Panico,[2a] Giovanni Sindona,*[2b] and Nicola Uccella[2b]**

*Contribution from the Department of Biochemistry, Imperial College, London S.W.7, England, and Dipartimento di Chimica, Università della Calabria, 87030-Arcavacata di Rende (CS), Italy.*
*Received September 30, 1982*

**Abstract:** Both the structure and sequence of DNA segments are determined by mass spectrometry (MS). Unprotected deoxyoligonucleotide triethylammonium salts TACC (**1**) and GGTA (**2**) have been directly analyzed from their aqueous solution by fast-atom-bombardment mass spectrometry (FABMS), with the aid of the MS/MS analytical approach. The desorbed gaseous oligomers are negative monocharged ions and possess a zwitterionic structure with three phosphodiester anionic moieties and two protonated bases. Sequence information can be derived both from the FAB-induced mass spectra of primary and metastable ions (MI) and the collisional activation (CA) secondary ions.

## Introduction

DNA segments from both synthetic and natural sources can be sequenced after chemical or enzymatic degradation by conventional chromatographic techniques.[3] Fast-atom-bombardment mass spectrometry (FABMS), originally introduced for otherwise intractable molecules,[4] has been recently applied to determine the structure and chemistry of deoxyoligonucleotide salts, sampled from their water solution into a glycerol matrix and analyzed in the negative mode, after sputtering caused by a 6-keV argon atom beam.[5] The introduction of ionization procedures alternative to the classic electron impart (EI)[6] appears to have overcome an original drawback of mass spectrometry, i.e., the volatilization of polar[5,7] and extremely large molecules.[8] However, the lower abundances of information-bearing fragment ions often produced represents a severe limitation to the employment of those soft methods for other than molecular weight determination.

Fast atom bombardment of organic molecules dissolved in viscous matrixes usually provides sufficient structural information by the appearance of diagnostic fragments in the spectra of the primary ions thus produced. The observed electron-impact-like behavior, the simplicity of sample preparation and manipulation, and, last but not least, the availability of commercial FAB guns have promoted an extensive application of the technique in the structure elucidation of complex biomolecules. However, no definite theoretical models have yet been proposed to explain the ionization mechanism of very large molecules by particle-induced desorption, while some "hidden variables" seem to affect the obtainment of the spectra.[6b] Therefore, if this approach is applied to the analysis of unblocked DNAs, much attention has to be paid to the rationalization of the eventually observed fragmentation pattern. Furthermore, the biological important pieces of information stored in a oligodeoxyribonucleotide are a function of the sequence of only four chemical variables, i.e., the cytidine, thy-

(1) Work supported by Progetto Finalizzato del CNR—Chimica Fine e Secondaria. For part 2, see ref 10.
(2) (a) Imperial College. On leave absence from Università della Calabria. (b) Università della Calabria.
(3) Tu, C. D.; Wu, R. "Methods in Enzymology"; Academic Press: New York, 1980; Vol. 65, Part I, p 620.
(4) Barber, M.; Bordoli, R. S.; Sedgwick, R. D.; Tyler, A. N. *Nature (London)* **1981**, *293*, 270.
(5) Sindona G.; Uccella, N.; Weclawek, K. *J. Chem. Res., (S)* **1982**, 184.
(6) (a) Macfarlane, R. D.; Togerson, D. F. *Science* **1976**, *191*, 920. (b) Macfarlane, R. D. *Acc. Chem. Res.* **1982**, *15*, 268.
(7) Morris, H. R.; Panico, M.; Barber, M.; Bordoli, R. S.; Sedgwick, R. D.; Tyler, A. Biochem. Biophys. Res. Commun. **1981**, *101*, 623.
(8) McNeal, C. J.; Macfarlane, R. D. *J. Am. Chem. Soc.* **1981**, *103*, 1609.

0002-7863/83/1505-5607$01.50/0 